

Light harvesting complex LH2 - simulation of spectral profiles

Pavel Heřman, and David Zapletal

Abstract— Absorption and steady state fluorescence spectra are simulated for relatively simple circular molecular system. It can be treated as a model of peripheral light harvesting complex LH2 from purple bacterium *Rhodospseudomonas acidophila*. Both rings (B850 ring and B800 one) are included in our model. The spectra are calculated within full Hamiltonian model and compared for two types of slow fluctuations. Gaussian fluctuations in local excitations energies and Gaussian fluctuations in positions of bacteriochlorophylls are considered. Fast fluctuations, interaction with phonon bath, is also taking into account for low and room temperature. The resulting spectra show strong dependence on temperature. Splitting of both spectra are visible at low temperature. The differences caused by static disorder type are also remarkable. Localization of exciton states contributing to the steady state fluorescence spectra is investigated by thermally averaged by participation ratio.

Keywords—LH2, B800 ring, B850 ring, absorption and fluorescence spectrum, static and dynamic disorder, exciton states, localization

I. INTRODUCTION

THE antenna systems of photosynthetic units from purple bacteria are formed by ring light harvesting (LH) complexes LH1, LH2, LH3, and LH4. Their geometric structures are known in great detail from X-ray crystallography [1-5]. The general organization of above mentioned light-harvesting complexes is the same: identical subunits are repeated cyclically in such a way that a ring-shaped structure is formed. However the symmetries of these rings are different.

The bacteriochlorophyll (BChl) molecules from LH2 complex in purple bacterium *Rhodospseudomonas acidophila* are organized in two concentric rings. One ring features a group of nine well-separated BChl molecules (B800) with absorption band at about 800 nm. The other ring consists of eighteen closely packed BChl molecules (B850) absorbing around 850 nm. As in B850 ring as in B800 ring dipole moments of BChl molecules are oriented approximately tangentially to corresponding ring. While the nearest neighbour dipole moments in B850 ring have antiparallel arrangement, in B800 ring the orientations of the nearest neighbour dipole moments are parallel [6]. LH2 complexes from other purple bacteria have analogous ring structure.

Some bacteria express also other types of complexes such as

the B800-820 LH3 complex (*Rhodospseudomonas acidophila* strain 7050) or the LH4 complex (*Rhodospseudomonas palustris*). LH3 complex like LH2 one is usually nonameric but LH4 one is octameric. The other difference is the presence of an additional BChl ring in LH4 complex [3]. Different arrangements manifest themselves in different optical properties. At this article we mainly focus on LH2 complex.

Despite intensive study of bacterial antenna systems the precise role of the protein moiety for governing the dynamics of the excited states is still under debate. At room temperature the solvent and protein environment fluctuates with characteristic time scales ranging from femtoseconds to nanoseconds. The simplest approach is to substitute fast fluctuations by dynamic disorder and slow fluctuations by static disorder.

In our previous papers we presented results of simulations for B850 ring from LH2 complex. In several steps we extended the former investigations of static disorder effect on the anisotropy of fluorescence made by Kumble and Hochstrasser [7] and Nagarajan et al. [8-10] for LH2 ring. After studying the influence of diagonal dynamic disorder for simple systems (dimer, trimer) [11-13], we added this effect into our model of LH2 ring by using a quantum master equation in Markovian and non-Markovian limits [14-17]. We also studied influence of four types of uncorrelated static disorder [18,19] (Gaussian disorder in local excitation energies, Gaussian disorder in transferintegrals, Gaussian disorder in radial positions of BChls and Gaussian disorder in angular positions of BChls on the ring). Influence of correlated static disorder, namely an elliptical deformation of the ring, was taken into account too [15]. We also investigated the time dependence of fluorescence anisotropy for the LH4 ring with different types of uncorrelated static disorder [19,20].

Recently we have focused on the modeling of absorption and steady state fluorescence spectra. Our results for B850 ring from LH2 complex and B- α /B- β ring from LH4 complex within the nearest neighbour approximation model have been presented in [21-25]. The results within full Hamiltonian model were published in [26-34]. Very recently we have started to investigate the nearest neighbour transferintegral distributions for various types of static disorder connected with fluctuations in ring geometry of B850 ring from LH2 complex [35-38].

Main goal of the present paper is the extension of our previous investigation of absorption and steady state

This work was supported in part by the Faculty of Science, University of Hradec Králové (project of specific research No. 2104/2018 - P. Heřman)

fluorescence spectra to the whole LH2 complex (B850 ring and B800 one) and static disorder in geometry of modeled system.

The rest of the paper is structured as follows. Section II introduces our model of LH2 complex with two types of static disorder. Used units and parameters can be found in Section III. Results are presented and discussed in Section IV and conclusions are drawn in Section V.

II. MODEL

Only one exciton is assumed to be present in our model of LH2 complex after an impulsive excitation. The hamiltonian of an exciton in the molecular complex is composed from four terms,

$$H = H_{\text{ex}}^0 + H_s + H_{\text{ph}} + H_{\text{ex-ph}}. \quad (1)$$

A. Ideal Complex

The first term in (1),

$$H_{\text{ex}}^0 = \sum_{m,n(m \neq n)} J_{m,n} \hat{a}_m^\dagger \hat{a}_n, \quad (2)$$

describes an exciton in the ideal system (e.g. in the complex without any disorder). The operator \hat{a}_m^\dagger (\hat{a}_m) creates (annihilates) an exciton at site m , $J_{m,n}$ (for $m \neq n$) is the so-called transferintegral between sites m and n . It gives the strength of interaction between these sites. The arrangement of dipole moments in our model of LH2 system (see Fig. 1) gives us following relationship between transferintegrals:

$$J_{m,n}^{\text{B850}} = J_{m+k,n+k}^{\text{B850}}, \quad m, n, m+k, n+k = 1, \dots, 18, \quad (3)$$

$$J_{m,n}^{\text{B800}} = J_{m+k,n+k}^{\text{B800}}, \quad m, n, m+k, n+k = 19, \dots, 27. \quad (4)$$

The nearest neighbour transferintegral $J_{m,m+1}^{\text{B850}}$ in B850 ring is marked as J_0 and the nearest neighbour transferintegral $J_{m,m+1}^{\text{B800}}$ in B800 ring as J_1 . Their signs are given by the orientations of corresponding dipole moments [6], i.e. J_0 is positive and J_1 is negative. The relation between them is

$$J_1 \doteq -0.1J_0, \quad (5)$$

according to [6]. Each bacteriochlorophyll from B800 ring has two nearest neighbour bacteriochlorophylls from B850 ring. The transferintegrals $J_{1,19}$ and $J_{2,19}$ that connect these BChls from both rings have opposite signs and their values are approximately [6]

$$J_{1,19} = J_{3,20} = \dots = J_{17,27} \doteq 0.1J_0, \quad (6)$$

$$J_{2,19} = J_{4,20} = \dots = J_{18,27} \doteq -0.03J_0. \quad (7)$$

The dipole--dipole approximation,

$$J_{m,n} = \frac{\vec{d}_m \cdot \vec{d}_n}{|\vec{r}_{m,n}|^3} - 3 \frac{(\vec{d}_m \cdot \vec{r}_{m,n})(\vec{d}_n \cdot \vec{r}_{m,n})}{|\vec{r}_{m,n}|^5} = |\vec{d}_m| |\vec{d}_n| \frac{\cos \varphi_{m,n} - 3 \cos \varphi_m \cos \varphi_n}{|\vec{r}_{m,n}|^3}, \quad (8)$$

which is considered by us, and the relations between J_0 , J_1 , $J_{1,19}$ and $J_{2,19}$ give the geometry of our model of the whole

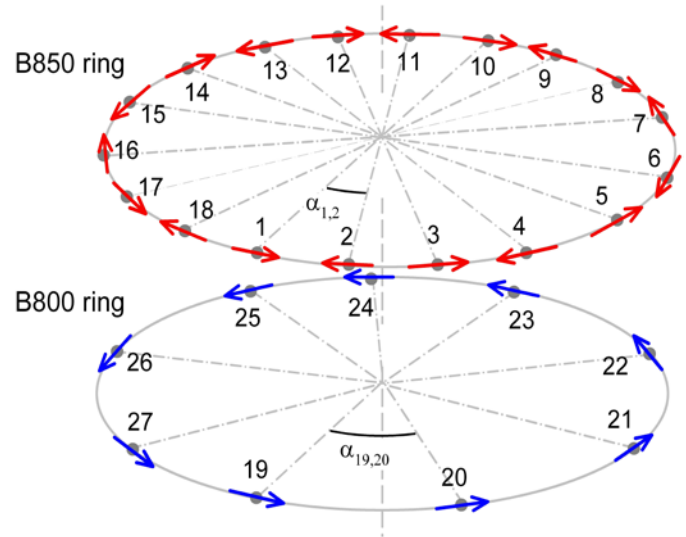


Fig. 1 Geometric arrangement of dipole moments in the ideal LH2 complex (without any fluctuations) dipole moments are oriented tangentially to the rings (B850 ring – red arrows: $\alpha_{m,m+1} = \pi/9$; B800 ring – blue arrows: $\alpha_{m,m+1} = 2\pi/9$)

complex. I.e. the ratio of the radii and the axial distance z_0 of both rings are

$$r_1 = 1.078r_0, \quad z_0 = 0.575r_0. \quad (9)$$

Here r_0 denotes the radius of B850 ring and r_1 the radius of B800 ring (see Fig. 1).

The pure exciton hamiltonian H_{ex}^0 can be diagonalized using the wave vector representation with corresponding delocalized Bloch states α and energies E_α . Using Fourier transformed excitonic operators \hat{a}_α , the Hamiltonian H_{ex}^0 in α -representation reads

$$H_{\text{ex}}^0 = \sum_{\alpha} E_{\alpha} \hat{a}_{\alpha}^{\dagger} \hat{a}_{\alpha}. \quad (10)$$

If we consider only one ring (B850 or B800) separately within the nearest neighbour approximation model (i.e. only the nearest neighbour bacteriochlorophylls are connected with nonzero transferintegrals $J_{m,n}$), the form of the operators \hat{a}_{α} in (10) is

$$\hat{a}_{\alpha} = \sum_{n=1}^N \hat{a}_n e^{i\alpha n}, \quad \alpha = \frac{2\pi}{N} l \quad (11)$$

and

$$E_{\alpha} = -2J_0 \cos \alpha. \quad (12)$$

Here

$$l = 0, \pm 1, \dots, \pm \frac{N}{2} \quad (13)$$

for even number of sites N (i.e. for B850 ring, where $N=18$) and

$$l = 0, \pm 1, \dots, \pm \frac{N-1}{2} \quad (14)$$

for odd number of sites N (i.e. for B800 ring, where $N=9$).

If both rings are considered simultaneously and all transferintegrals $J_{m,n}$ are considered to be nonzero, energetic

spectrum is more complex (see Fig. 2).

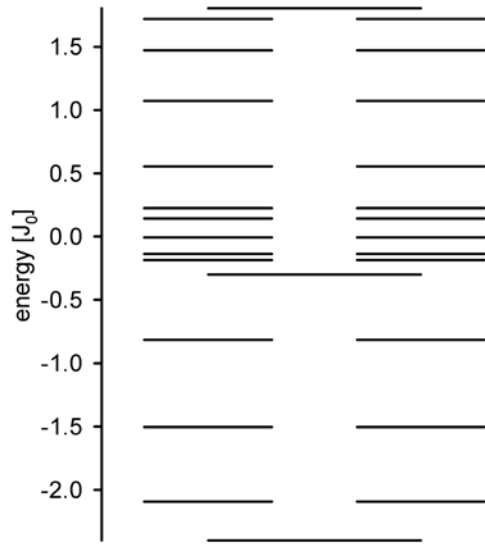


Fig. 2 Energetic spectrum of the whole LH2 complex (B850 ring and B800 ring) without any fluctuations

B. Static disorder

Influence of static disorder (second term in (1)) can be modeled by totally uncorrelated fluctuations of local excitation energies $\delta\varepsilon_n$ with Gaussian distribution and standard deviation Δ . Hamiltonian of static disorder H_s then reads

$$H_s = \sum_n \delta\varepsilon_n \hat{a}_n^\dagger a_n. \quad (15)$$

Another way to take into account such disorder is to model it as slow fluctuations in ring geometry. Deviation in ring geometry results in changes of transferintegrals $\delta J_{m,n}$ ($m \neq n$),

$$J_{m,n} = J_{n,m} = J_{m,n}^0 + \delta J_{m,n}. \quad (16)$$

Static disorder in ring geometry can be considered in two ways - fluctuations in molecular positions or fluctuations in molecular dipole moment orientations.

In the present paper we consider as fluctuations in local excitation energies (15) and the first above mentioned type of fluctuations in transferintegrals - fluctuations in molecular positions,

$$\vec{r}_n = \vec{r}_{n,0} + \delta\vec{r}_n, \quad n = 1, \dots, 27. \quad (17)$$

Here $\vec{r}_{n,0}$ and \vec{r}_n denote the position of n -th bacteriochlorophyll in ideal complex and disordered one and $\delta\vec{r}_n$ marks the displacement of m -th bacteriochlorophyll. The length of $\delta\vec{r}_n$ has Gaussian distribution with zero mean and standard deviation Δ_r , the direction of $\delta\vec{r}_n$ is distributed uniformly.

C. Dynamic Disorder

The third term in (1),

$$H_{ph} = \sum_q \hbar\omega_q b_q^\dagger b_q, \quad (18)$$

represents phonon bath in harmonic approximation (phonon creation and annihilation operators are denoted by b_q^\dagger and b_q , respectively).

Last term in (1),

$$H_{ex-ph} = \frac{1}{\sqrt{N}} \sum_n \sum_q G_q^n \hbar\omega_q \hat{a}_n^\dagger \hat{a}_n (\hat{b}_q^\dagger + \hat{b}_q), \quad (19)$$

describes exciton-phonon interaction which is assumed to be site-diagonal and linear in the bath coordinates (the term G_q^n denotes the exciton-phonon coupling constant).

D. Spectral Responses

Absorption $OD(\omega)$ and steady-state fluorescence $FL(\omega)$ spectra of the system with exciton-phonon coupling are calculated by the cumulant-expansion method of Mukamel et al. [39,40], i.e.

$$OD(\omega) = \omega \sum_\alpha d_\alpha^2 \operatorname{Re} \int_0^\infty dt e^{i(\omega - \omega_\alpha)t - g_{\alpha\alpha\alpha\alpha}t - R_{\alpha\alpha\alpha\alpha}t}, \quad (20)$$

$$FL(\omega) = \omega \sum_\alpha P_\alpha d_\alpha^2 \operatorname{Re} \int_0^\infty dt e^{i(\omega - \omega_\alpha)t + i\lambda_{\alpha\alpha\alpha\alpha}t - g_{\alpha\alpha\alpha\alpha}^*t - R_{\alpha\alpha\alpha\alpha}t}. \quad (21)$$

Here $\vec{d}_\alpha = \sum_n c_n^\alpha \vec{d}_n$ denotes the transition dipole moment of eigenstate α , c_n^α mark the expansion coefficients of the eigenstate α in site representation and P_α is the steady state population of the eigenstate α . The inverse lifetime of exciton state α is denoted $R_{\alpha\alpha\alpha\alpha}$ and it is given by a sum of the relaxation rates $R_{\beta\beta\alpha\alpha}$ between exciton states α , β , i.e. $R_{\alpha\alpha\alpha\alpha} = \sum_{\alpha \neq \beta} R_{\beta\beta\alpha\alpha}$ [41]. $R_{\beta\beta\alpha\alpha}$ are the elements of Redfield tensor $R_{\alpha\beta\gamma\delta}$ [42]. The g -function and λ -values in (20), (21) read

$$g_{\alpha\beta\gamma\delta} = - \int_{-\infty}^{\infty} \frac{d\omega}{2\pi\omega^2} C_{\alpha\beta\gamma\delta}(\omega) \times \left[\coth \frac{\omega}{2k_B T} (\cos \omega t - 1) - i(\sin \omega t - \omega t) \right], \quad (22)$$

$$\lambda_{\alpha\beta\gamma\delta} = - \lim_{t \rightarrow \infty} \frac{d}{dt} \operatorname{Im} \{ g_{\alpha\beta\gamma\delta}(t) \} = \int_{-\infty}^{\infty} \frac{d\omega}{2\pi\omega} C_{\alpha\beta\gamma\delta}(\omega). \quad (23)$$

The matrix of spectral densities $C_{\alpha\beta\gamma\delta}(\omega)$ in the eigenstate (exciton) representation reflects one-exciton states coupling to the manifold of phonon modes. In what follows only a diagonal exciton phonon interaction in site representation is used (see (19)), i.e., only fluctuations of the pigment site energies are assumed and the restriction to the completely uncorrelated dynamic disorder is applied. Each site (i.e. each chromophore) has its own bath completely uncoupled from the baths of the other sites in such case. Furthermore it is assumed that these baths have identical properties [16,43,44]. Then we need only one spectral density $C(\omega)$. The matrix of spectral

densities has the form

$$C_{mm'n'}(\omega) = \delta_{mn} \delta_{nm'} \delta_{m'n} C(\omega) \quad (24)$$

in site representation and

$$C_{\alpha\beta\gamma\delta}(\omega) = \sum_n c_n^\alpha c_n^\beta c_n^\gamma c_n^\delta C(\omega) \quad (25)$$

in the exciton representation.

From various models of spectral density $C(\omega)$ of the bath [41,45,46] we have used the model of Kühn and May [45]

$$C(\omega) = \theta(\omega) j_0 \frac{\omega^2}{2\omega_c^3} e^{-\frac{\omega}{\omega_c}} \quad (26)$$

which has its maximum at $2\omega_c$.

Localization of the exciton states contributing to the steady state fluorescence spectrum $FL(\omega)$ can be characterized by the thermally averaged participation ratio $\langle PR \rangle$, which is given by

$$\langle PR \rangle = \frac{\sum_\alpha PR_\alpha e^{-\frac{E_\alpha}{kT}}}{\sum_\alpha e^{-\frac{E_\alpha}{kT}}}, \quad (27)$$

where quantity

$$PR_\alpha = \sum_{n=1}^N |c_n^\alpha|^4 \quad (28)$$

gives information about localization of eigenstate α . Higher value of participation ratio PR_α corresponds to higher localization of this eigenstate and similarly higher value of $\langle PR \rangle$ corresponds to higher localization of exciton states contributing to the spectrum.

III. UNITS AND PARAMETERS

Energies normalized to the transferintegral J_0 (the nearest

neighbour transferintegral in B850 ring) have been used in our calculations. Estimation of J_0 varies in literature between 250 cm^{-1} and 400 cm^{-1} . In our previous investigations [47] we found from comparison with experimental results for B850 ring [48] that the possible strength Δ of the uncorrelated Gaussian static disorder in local excitation energies $\delta\varepsilon_n$ is approximately $\Delta \approx 0.30J_0$ and possible strength of the uncorrelated Gaussian static disorder in transferintegrals is approximately two times smaller. That is why we have taken the strengths Δ and Δ_r in following intervals:

$$\Delta \in \langle 0.10J_0, 0.60J_0 \rangle, \quad \Delta_r \in \langle 0.05r_0, 0.30r_0 \rangle. \quad (29)$$

All our simulations of LH2 spectra have been done with the same values of J_0 and unperturbed transition energy from the ground state E_0 ,

$$J_0 = 370 \text{ cm}^{-1}, \quad E_0 = 12280 \text{ cm}^{-1}, \quad (30)$$

that we found for the B850 ring only and for static disorder in local excitation energies [49]. All our calculations have been done for 4000 realizations of corresponding type of static disorder.

In agreement with our previous results [18,50] we have used the strength of dynamic disorder $j_0 = 0.4J_0$ and cut-off frequency $\omega_c = 0.212J_0$ (see (26)).

IV. RESULTS AND DISCUSSION

Absorption OD and steady state fluorescence FL spectra are calculated for full LH2 complex (B850 ring and B800 one). Two types of uncorrelated static disorder (Gaussian fluctuations in local excitation energies $\delta\varepsilon_n$ and Gaussian fluctuations in positions of bacteriochlorophylls $\delta\vec{r}_n$ are taken

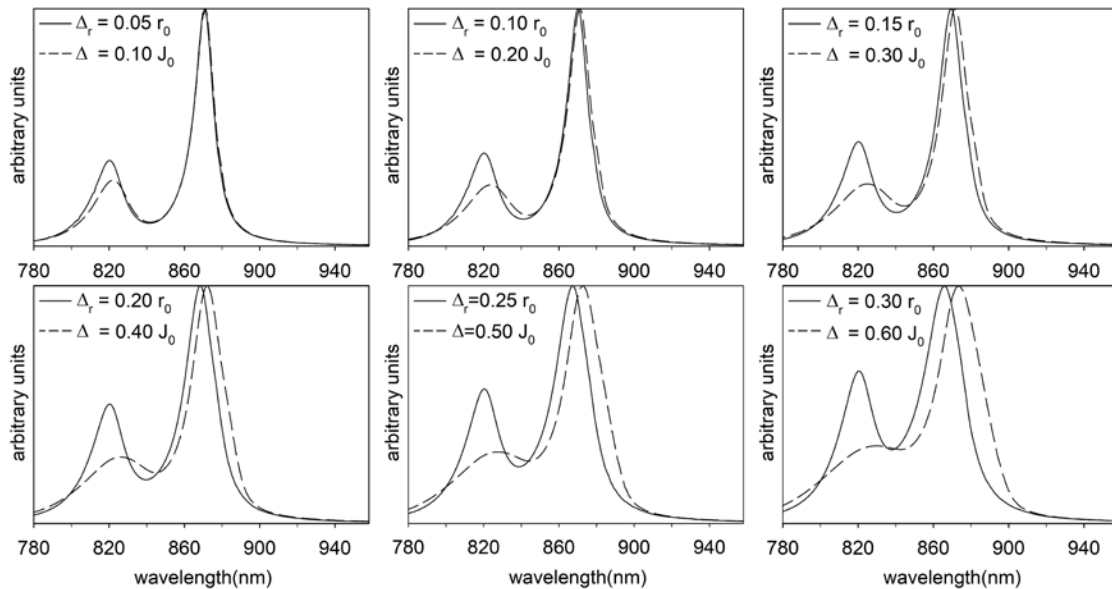


Fig. 3 Calculated absorption spectral profiles $OD(\lambda)$ (arbitrary units) for the whole LH2 complex (B850 ring and B800 ring) at low temperature $kT = 0.1J_0$ averaged over 4000 realizations of uncorrelated static disorder (six strengths, fluctuations in positions of bacteriochlorophylls $\delta\vec{r}_n$ - solid lines, fluctuations in local excitation energies $\delta\varepsilon_n$ - dashed lines).

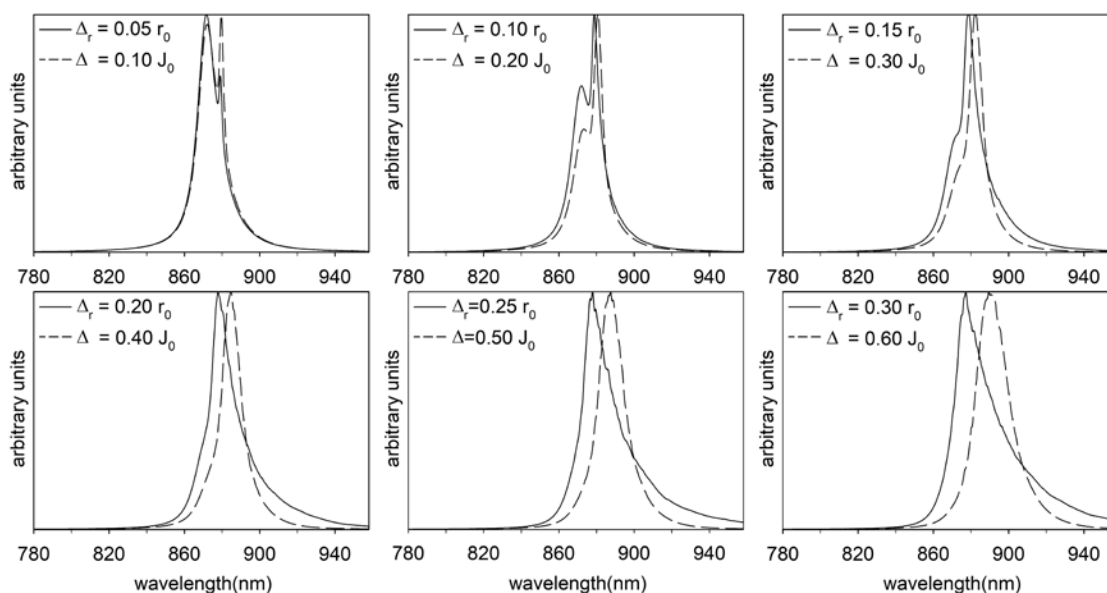


Fig. 4 Calculated steady state fluorescence spectral profiles $FL(\lambda)$ (arbitrary units) for the whole LH2 complex (B850 ring and B800 ring) at low temperature $kT = 0.1J_0$ averaged over 4000 realizations of uncorrelated static disorder (six strengths, fluctuations in positions of bacteriochlorophylls $\delta\vec{r}_n$ - solid lines, fluctuations in local excitation energies $\delta\epsilon_n$ - dashed lines).

into account in our simulations simultaneously with dynamic disorder in Markovian approximation.

Resulting absorption OD and steady state fluorescence FL spectral profiles as functions of wavelength λ can be seen in Fig. 3 ($OD(\lambda)$ spectrum) and in Fig. 4 ($FL(\lambda)$ spectrum) for

low temperature $kT = 0.1J_0$. Here k is the Boltzmann constant. The same spectra for room temperature $kT = 0.5J_0$ are presented in Fig. 5 ($OD(\lambda)$ spectrum) and Fig. 6 ($FL(\lambda)$ spectrum). The influence of above mentioned two types of static disorder on spectral profiles is compared in each

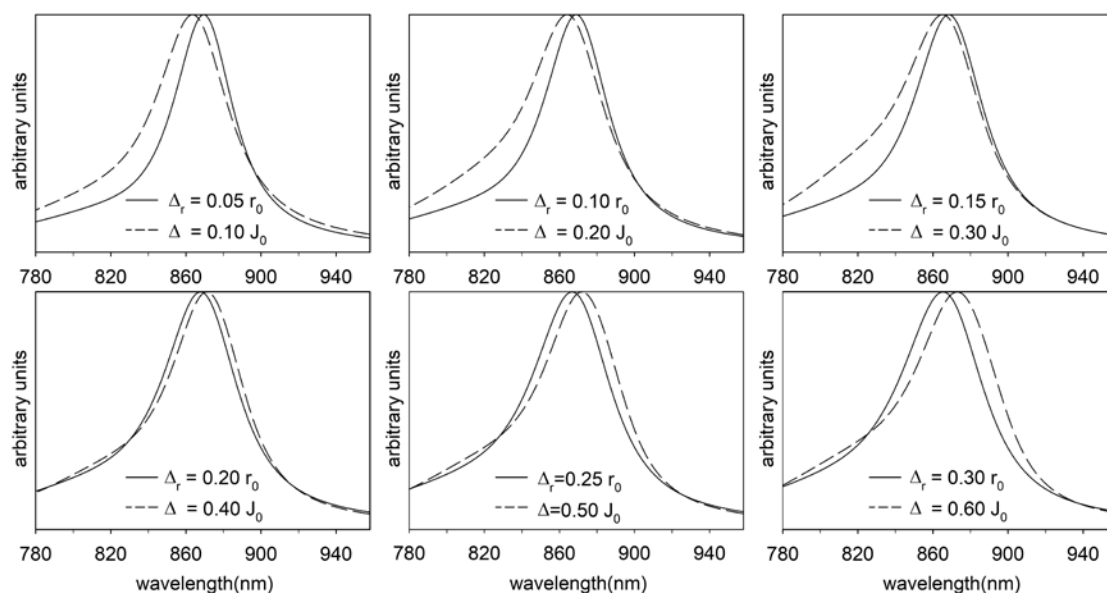


Fig. 5 Calculated absorption spectral profiles $OD(\lambda)$ (arbitrary units) for the whole LH2 complex (B850 ring and B800 ring) at room temperature $kT = 0.5J_0$ averaged over 4000 realizations of uncorrelated static disorder (six strengths, fluctuations in positions of bacteriochlorophylls $\delta\vec{r}_n$ - solid lines, fluctuations in local excitation energies $\delta\epsilon_n$ - dashed lines).

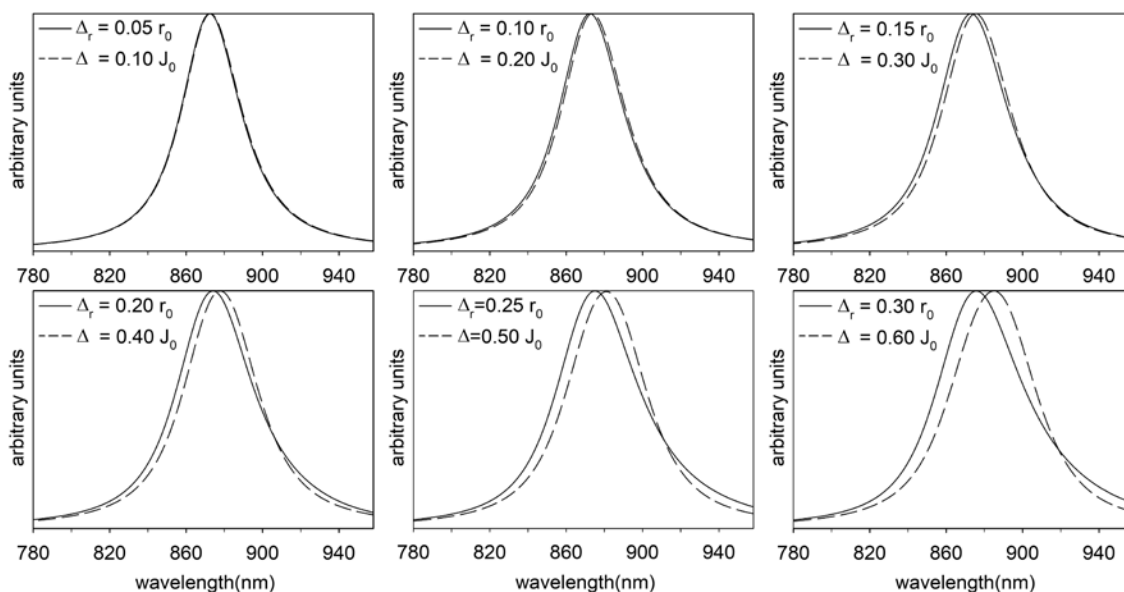


Fig. 6 Calculated steady state fluorescence spectral profiles $FL(\lambda)$ (arbitrary units) for the whole LH2 complex (B850 ring and B800 ring) at room temperature $kT = 0.5J_0$ averaged over 4000 realizations of uncorrelated static disorder (six strengths, fluctuations in positions of bacteriochlorophylls $\delta\vec{r}_n$ - solid lines, fluctuations in local excitation energies $\delta\epsilon_n$ - dashed lines).

presented figure.

The distributions of the thermally averaged participation ratio $\langle PR \rangle$ at low temperature ($kT = 0.1J_0$) are shown in Fig. 7 for the static disorder in local excitation energies $\delta\epsilon_n$ and in Fig. 8 for the static disorder in positions of molecules $\delta\vec{r}_n$.

The same at room temperature ($kT = 0.5J_0$) is presented in Fig. 9 and Fig. 10.

In case of absorption spectrum $OD(\lambda)$ at low temperature ($kT = 0.1J_0$, Fig 3) the shift of spectral profile maxima with growing static disorder strength is present. As concerns the

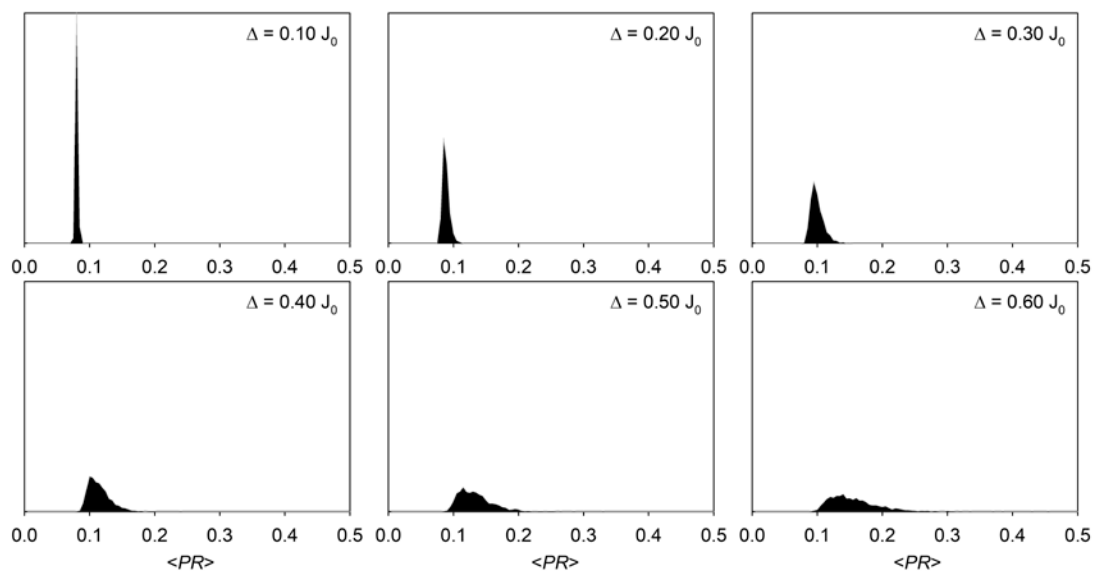


Fig. 7 The distributions of the thermally averaged participation ratio $\langle PR \rangle$ calculated for the whole LH2 complex (B850 ring and B800 ring) at low temperature $kT = 0.1J_0$ for 4000 realizations of uncorrelated static disorder in local excitation energies $\delta\epsilon_n$.

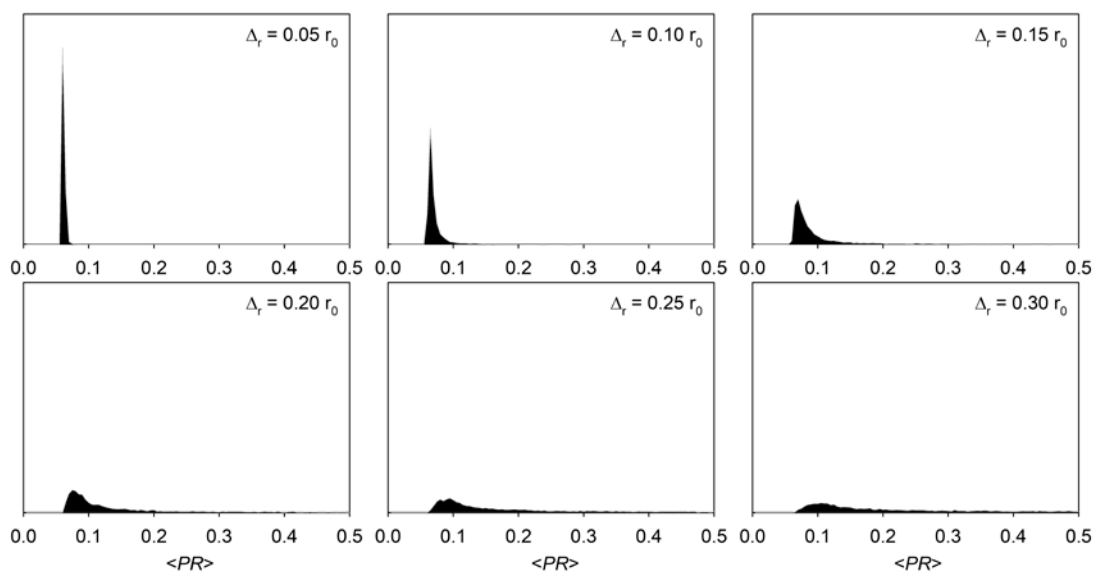


Fig. 8 The distributions of the thermally averaged participation ratio $\langle PR \rangle$ calculated for the whole LH2 complex (B850 ring and B800 ring) at low temperature $kT = 0.1J_0$ for 4000 realizations of uncorrelated static disorder in the positions of bacteriochlorophylls $\delta\vec{r}_n$.

maximum which corresponds B850 ring (right hand side maximum), we can see the shift in opposite directions for different types of static disorder. In case of the fluctuations in local excitation energies $\delta\epsilon_n$ the maximum shifts to higher wavelengths in comparison with the case of the fluctuations in positions $\delta\vec{r}_n$ of bacteriochlorophylls where the maximum is shifted to lower wavelengths. The maximum which corresponds B800 ring (left hand side one) shifts to higher wavelengths for static disorder $\delta\epsilon_n$ and it does not shift

significantly for the static disorder $\delta\vec{r}_n$.

If the peak height ratios (B850/B800) are compared, we can see diminishing ratio with growing static disorder strength for both types of static disorder. But this ratio diminishes much more for the static disorder $\delta\vec{r}_n$ in comparison with static disorder $\delta\epsilon_n$.

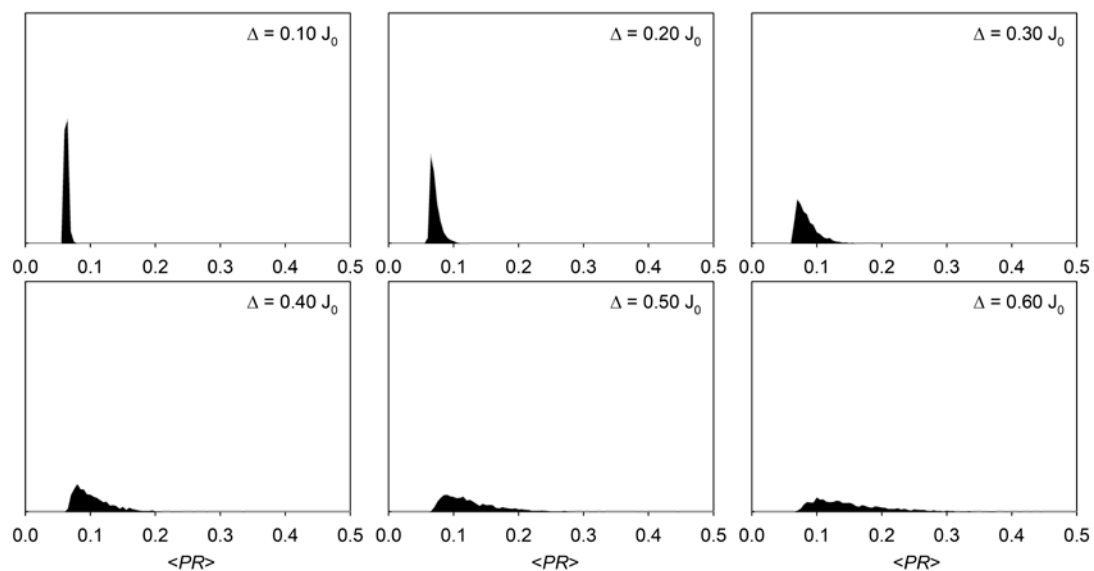


Fig. 9 The distributions of the thermally averaged participation ratio $\langle PR \rangle$ calculated for the whole LH2 complex (B850 ring and B800 ring) at room temperature $kT = 0.5J_0$ for 4000 realizations of uncorrelated static disorder in local excitation energies $\delta\epsilon_n$.

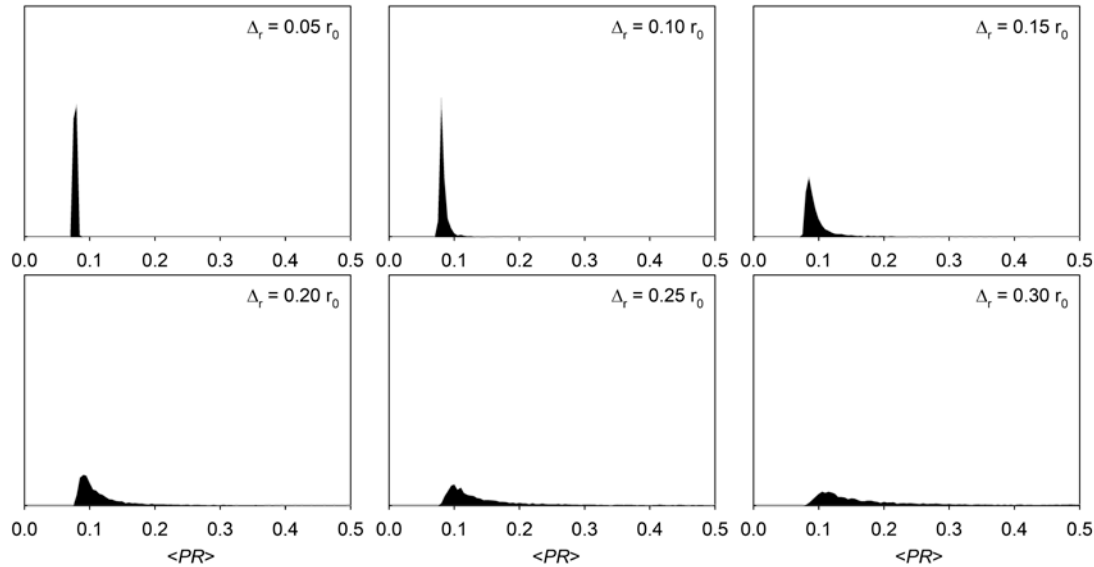


Fig. 10 The distributions of the thermally averaged participation ratio $\langle PR \rangle$ calculated for the whole LH2 complex (B850 ring and B800 ring) at room temperature $kT = 0.5J_0$ for 4000 realizations of uncorrelated static disorder in the positions of bacteriochlorophylls $\delta\vec{r}_n$.

Fluorescence spectra $FL(\lambda)$ at low temperature (Fig. 4) also show two peaks especially for lower static disorder strengths. But contrary to absorption spectra, these maxima are not connected with different rings. They are also present in fluorescence spectral profile of B850 ring only [26]. As concerns spectral profile widths, they are larger for higher static disorder strengths (both types of static disorder). Significant peak shift to higher wavelengths is present only in case of the static disorder $\delta\epsilon_n$. On the other hand, pronounced right spectral tail can be seen in case of the static disorder $\delta\vec{r}_n$.

Dynamic disorder depends on temperature and its influence at room temperature ($kT = 0.5J_0$) is higher. Peaks are wider and overlap. That is why only one peak is present in both spectral profiles ($OD(\lambda)$ and $FL(\lambda)$) in case of room temperature $kT = 0.5J_0$ (see Fig. 5 and Fig. 6). Both spectral profiles become wider for growing strength of static disorder regardless of its type. The peak of absorption spectrum shifts to higher wavelengths for higher strength of static disorder $\delta\epsilon_n$ in comparison with static disorder $\delta\vec{r}_n$, where the peak slightly shifts to lower wavelengths. The peak position of fluorescence spectrum varies only in case of static disorder $\delta\epsilon_n$. It again shifts to higher wavelengths.

As concerns localization of exciton states contributing to steady state fluorescence spectra, the distributions of participation ratio $\langle PR \rangle$ are wider at room temperature $kT = 0.5J_0$ than at low temperature $kT = 0.1J_0$. It indicates larger contribution of the exciton states with higher localization at room temperature for both types of static disorder. We can see the shift of the distribution maximum to

higher values of $\langle PR \rangle$ for growing strength of static disorder. This shift is more noticeable in case of the static disorder in positions of bacteriochlorophylls $\delta\vec{r}_n$. It means that the contribution of localized exciton states increases faster for this type of static disorder.

V. CONCLUSIONS

From our new results for full LH2 complex and comparison with our previous results we can make following conclusions.

At low temperature ($kT = 0.1J_0$) two strong peaks of absorption spectral profiles corresponding B850 ring and B800 one are visible for both presented types of static disorder. Fluorescence spectra at low temperature also show splitting especially for lower static disorder strengths but this splitting does not come from the individual B850 ring and B800 ring. At room temperature ($kT = 0.5J_0$) no splitting is visible as in absorption spectra as in fluorescence ones. It is caused by higher influence of dynamic disorder. Exciton states contributing to fluorescence spectra are more localized in case of room temperature.

Remarkable differences between presented static disorder types are in peak positions. The peaks of both spectral profiles significantly shift to higher wavelengths with growing strength of static disorder in local excitation energies. On the other hand, peak positions are slightly shifted to lower wavelengths or they do not show any change in case of static disorder in positions of bacteriochlorophylls. The localization of exciton states contribution to fluorescence spectrum grows faster in case of static disorder in positions of bacteriochlorophylls.

REFERENCES

- [1] G. McDermott, et al., "Crystal structure of an integral membrane lightharvesting complex from photosynthetic bacteria," *Nature*, vol. 374, pp. 517–521, 1995.
- [2] M. Z. Papiz, S. M. Prince, T. Howard, R. J. Cogdell, and N. W. Isaacs, "The structure and thermal motion of the B800–850 LH2 complex from *Rps. acidophila* at 2.0 Å resolution and 100 K: new structural features and functionally relevant motions," *J. Mol. Biol.*, vol. 326, pp. 1523–1538, 2003.
- [3] W. P. F. de Ruijter, et al., "Observation of the Energy-Level Structure of the Low-Light Adapted B800 LH4 Complex by Single-Molecule Spectroscopy," *Biophys. J.*, vol. 87, pp. 3413–3420, 2004.
- [4] A.W. Roszak, et al., "Crystal structure of RCLH1 core complex from *Rhodospseudomonas palustris*," *Science*, vol. 203, pp. 1969–1972, 2003.
- [5] K. McLuskey, S. M. Prince, R. J. Cogdell, and N. W. Isaacs, "The crystallographic structure of the B800-820 LH3 light-harvesting complex from the purple bacteria *Rhodospseudomonas acidophila* strain 7050," *Biochemistry*, vol. 40, pp. 8783–8789, 2001.
- [6] O. Kühn, V. Sundström, and T. Pullerits, "Fluorescence Depolarization Dynamics in the B850 Complex of Purple Bacteria," *Chem. Phys.*, vol. 275, pp. 15–30, 2002.
- [7] R. Kumble, and R. Hochstrasser, "Disorder-induced exciton scattering in the light-harvesting systems of purple bacteria: Influence on the anisotropy of emission and band ! band transitions," *J. Chem. Phys.*, vol. 109, pp. 855–865, 1998.
- [8] V. Nagarajan, R. G. Alden, J. C. Williams, and W. W. Parson, "Ultrafast exciton relaxation in the B850 antenna complex of *Rhodobacter sphaeroides*," *Proc. Natl. Acad. Sci. USA*, vol. 93, pp. 13774–13779, 1996.
- [9] V. Nagarajan, E. T. Johnson, J. C. Williams, and W. W. Parson, "Femtosecond pump-probe spectroscopy of the B850 antenna complex of *Rhodobacter sphaeroides* at room temperature," *J. Phys. Chem. B*, vol. 103, pp. 2297–2309, 1999.
- [10] V. Nagarajan, and W. W. Parson, "Femtosecond fluorescence depletion anisotropy: Application to the B850 antenna complex of *Rhodobacter sphaeroides*," *J. Phys. Chem. B*, vol. 104, pp. 4010–4013, 2000.
- [11] V. Čápek, I. Barvík, and P. Heřman, "Towards proper parametrization in the exciton transfer and relaxation problem: dimer," *Chem. Phys.*, vol. 270, pp. 141–156, 2001.
- [12] P. Heřman, and I. Barvík, "Towards proper parametrization in the exciton transfer and relaxation problem. II. Trimer," *Chem. Phys.*, vol. 274, pp. 199–217, 2001.
- [13] P. Heřman, I. Barvík, and M. Urbanec, "Energy relaxation and transfer in excitonic trimer," *J. Lumin.*, vol. 108, pp. 85–89, 2004.
- [14] P. Heřman, U. Kleinekathöfer, I. Barvík, and M. Schreiber, "Exciton scattering in light-harvesting systems of purple bacteria," *J. Lumin.*, vol. 94-95, pp. 447–450, 2001.
- [15] P. Heřman, and I. Barvík, "Non-Markovian effects in the anisotropy of emission in the ring antenna subunits of purple bacteria photosynthetic systems," *Czech. J. Phys.*, vol. 53, pp. 579–605, 2003.
- [16] P. Heřman, U. Kleinekathöfer, I. Barvík, and M. Schreiber, "Influence of static and dynamic disorder on the anisotropy of emission in the ring antenna subunits of purple bacteria photosynthetic systems," *Chem. Phys.*, vol. 275, pp. 1–13, 2002.
- [17] P. Heřman, and I. Barvík, "Temperature dependence of the anisotropy of fluorescence in ring molecular systems," *J. Lumin.*, vol. 122–123, pp. 558–561, 2007.
- [18] P. Heřman, and I. Barvík, "Coherence effects in ring molecular systems," *Phys. Stat. Sol. C*, vol. 3, pp. 3408–3413, 2006.
- [19] P. Heřman, D. Zapletal, and I. Barvík, "The anisotropy of fluorescence in ring units III: Tangential versus radial dipole arrangement," *J. Lumin.*, vol. 128, pp. 768–770, 2008.
- [20] P. Heřman, I. Barvík, and D. Zapletal, "Computer simulation of the anisotropy of fluorescence in ring molecular systems: Tangential vs. radial dipole arrangement," *Lecture Notes in Computer Science*, vol. 5101, pp. 661–670, 2008.
- [21] P. Heřman, D. Zapletal, and J. Šlégr, "Comparison of emission spectra of single LH2 complex for different types of disorder," *Phys. Proc.*, vol. 13, pp. 14–17, 2011.
- [22] D. Zapletal, and P. Heřman, "Simulation of molecular ring emission spectra: localization of exciton states and dynamics," *Int. J. Math. Comp. Sim.*, vol. 6, pp. 144–152, 2012.
- [23] M. Horák, P. Heřman, and D. Zapletal, "Simulation of molecular ring emission spectra - LH4 complex: localization of exciton states and dynamics," *Int. J. Math. Comp. Sim.*, vol. 7, pp. 85–93, 2013.
- [24] M. Horák, P. Heřman, and D. Zapletal, "Modeling of emission spectra for molecular rings - LH2, LH4 complexes," *Phys. Proc.*, vol. 44, pp. 10–18, 2013.
- [25] P. Heřman, and D. Zapletal, "Intermolecular coupling fluctuation effect on absorption and emission spectra for LH4 ring," *Int. J. Math. Comp. Sim.*, vol. 7, pp. 249–257, 2013.
- [26] P. Heřman, D. Zapletal, and M. Horák, "Emission spectra of LH2 complex: full Hamiltonian model," *Eur. Phys. J. B*, vol. 86, art. no. 215, 2013.
- [27] D. Zapletal, and P. Heřman, "Photosynthetic complex LH2 – absorption and steady state fluorescence spectra," in *Proc. of 6th Int. Conf. On Sust. Energy and Env. Protection (SEEP2013)*, Maribor: University of Maribor, 2013, pp. 284–290.
- [28] P. Heřman, and D. Zapletal, "Emission Spectra of LH4 Complex: Full Hamiltonian Model," *Int. J. Math. Comp. Sim.*, vol. 7, pp. 448–455, 2013.
- [29] P. Heřman, and D. Zapletal, "Simulation of Emission Spectra for LH4 Ring: Intermolecular Coupling Fluctuation Effect," *Int. J. Math. Comp. Sim.*, vol. 8, pp. 73–81, 2014.
- [30] D. Zapletal, and P. Heřman, "Photosynthetic complex LH2 - Absorption and steady state fluorescence spectra," *Energy*, vol. 77, pp. 212–219, 2014.
- [31] P. Heřman, and D. Zapletal, "Computer Simulation of Emission and Absorption Spectra for LH2 Ring," *Computational Problems in Science and Engineering, Lecture Notes in Electrical Engineering*, vol. 343, pp. 221–234, 2015.
- [32] P. Heřman, and D. Zapletal, "Modeling of Absorption and Steady State Fluorescence Spectra of Full LH2 Complex (B850 - B800 Ring)," *Int. J. Math. Mod. Meth. Appl. Sci.*, vol. 9, pp. 614–623, 2015.
- [33] P. Heřman, and D. Zapletal, "Modeling of Emission and Absorption Spectra of LH2 Complex (B850 and B800 Ring) - Full Hamiltonian Model," *Int. J. Math. Comp. Sim.*, vol. 10, pp. 208–217, 2016.
- [34] P. Heřman, and D. Zapletal, "B- α B- β Ring from Photosynthetic Complex LH4, Modeling of Absorption and Fluorescence Spectra," *Int. J. Math. Comp. Sim.*, vol. 10, pp. 332–344, 2016.
- [35] P. Heřman, and D. Zapletal, "B850 Ring from Photosynthetic Complex LH2 - Comparison of Different Static Disorder Types," *Int. J. Math. Comp. Sim.*, vol. 10, pp. 361–369, 2016.
- [36] P. Heřman, and D. Zapletal, "Fluctuations of Bacteriochlorophylls Positions in B850 Ring from Photosynthetic Complex LH2," *Int. J. Math. Comp. Sim.*, vol. 10, pp. 381–389, 2016.
- [37] P. Heřman, D. Zapletal, J. Loskot, and A. Hladíková, "Fluctuations of Pigments Dipole Moment Orientations in B850 Ring from Photosynthetic Complex LH2," *WSEAS Transactions on Appl. and Theor. Mech.*, vol. 12, pp. 105–112, 2017.
- [38] P. Heřman, and D. Zapletal, "B850 Ring from Light Harvesting Complex LH2 - Fluctuations in Dipole Moment Orientations of Bacteriochlorophyll Molecules," *Int. J. Biol. Biomed. Eng.*, vol. 11, pp. 39–47, 2017.
- [39] W. M. Zhang, T. Meier, V. Chernyak, and S. Mukamel, "Exciton migration and three-pulse femtosecond optical spectroscopies of photosynthetic antenna complexes," *J. Chem. Phys.*, vol. 108, pp. 7763–7774, 1998.
- [40] S. Mukamel, *Principles of nonlinear optical spectroscopy*, New York: Oxford University Press, 1995.
- [41] V. I. Novoderezhkin, D. Rutkauskas, and R. van Grondelle, "Dynamics of the emission spectrum of a single LH2 complex: Interplay of slow and fast nuclear motions," *Biophys. J.*, vol. 90, pp. 2890–2902, 2006.
- [42] A. G. Redfield, "The Theory of Relaxation Processes," *Adv. Magn. Reson.*, vol. 1, pp. 1–32, 1965.
- [43] D. Rutkauskas, V. Novoderezhkin, R. J. Cogdell, and R. van Grondelle, "Fluorescence spectroscopy of conformational changes of single LH2 complexes," *Biophys. J.*, vol. 88, pp. 422–435, 2005.
- [44] D. Rutkauskas, V. Novoderezhkin, R. J. Cogdell, and R. van Grondelle, "Fluorescence spectral fluctuations of single LH2 complexes from *Rhodospseudomonas acidophila* strain 10050," *Biochemistry*, vol. 43, pp. 4431–4438, 2004.
- [45] V. May, and O. Kühn, *Charge and Energy Transfer in Molecular Systems*. Berlin: Wiley-WCH, 2000.

- [46] O. Zerlauskiene, G. Trinkunas, A. Gall, B. Robert, and V. Urboniene, "Static and Dynamic Protein Impact on Electronic Properties of Light-Harvesting Complex LH2," *J. Phys. Chem. B*, vol. 112, pp. 15883–15892, 2008.
- [47] P. Heřman, I. Barvık, and D. Zapletal, "Energetic disorder and exciton states of individual molecular rings," *J. Lumin.*, vol. 119–120, pp. 496–503, 2006.
- [48] C. Hofmann, T. J. Aartsma, and J. Köhler, "Energetic disorder and the B850–exciton states of individual light–harvesting 2 complexes from *Rhodospseudomonas acidophila*," *Chem. Phys. Lett.*, vol. 395, pp. 373–378, 2004.
- [49] P. Heřman, D. Zapletal, and M. Horák, "Computer simulation of steady state emission and absorption spectra for molecular ring," in *Proc. 5th Int. Conf. on Advanced Engineering Computing and Applications in Sciences (ADVCOMP2011)*, Lisbon: IARIA, 2011, pp. 1–6.
- [50] P. Heřman, D. Zapletal, and I. Barvık, "Lost of coherence due to disorder in molecular rings," *Phys. Stat. Sol. C*, vol. 6, pp. 89–92, 2009.
- [51] P. Heřman, and D. Zapletal, "Modeling of Absorption and Steady State Fluorescence Spectra of Full LH2 Complex (B850 - B800 Ring)," *Int. J. Math. Models and Methods in Appl. Sci.*, vol. 9, pp. 614–623, 2015